Supplementary Information (SI) for Physical Chemistry Chemical Physics.

Electronic Supplementary Information

A new approach to a first order irreversible homogeneous chemical reaction followed by an electrochemical process (C_iE mechanism): theory, simulation and application

Rafael A. L. Chioquetti [a], Raphael P. Bacil[a], Silvia H. P. Serrano [a]

[a]Instituto de Química, Universidade de Sao Paulo - Av. Prof. Lineu Prestes, 748 - Butantã - São Paulo – SP, Brazil. CEP: 05508-000.

1. Simulations

In **Fig. S1**, although the chronoamperograms in pure Cottrell regime simulated with different time steps are almost identical, their semi-derivatives and semi-integrals with respect to time are different. While the theoretical semi-integral of a Cottrell profile would result a non-null constant, we see in the simulations that the graphs only tend to a constant after a while, and this condition is achieved faster for the shorter time step. The same considerations are valid for the semi-derivative plots, in which the calculated values should tend to 0.

These observations point out to the choice of adequate lengths of time steps as a crucial aspect for the accuracy and to the meaning of kinetic measures performed with chronoamperometry, as proposed in this work.

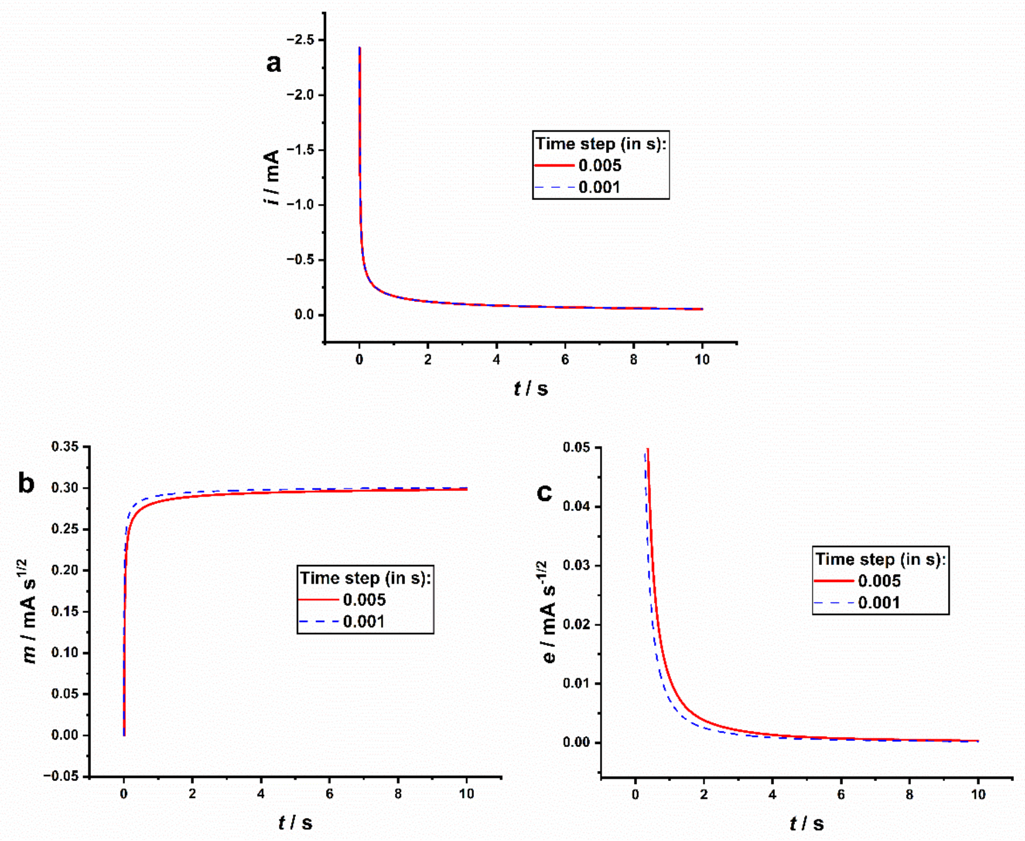

Fig. S1 Chronoamperograms simulated with $R_i = 0$ and $A_i = 1$ mmol L^{-1} **(a)** and their semi-integrals **(b)** and semi-derivatives **(c)** with respect to time. The time steps used are 0.005 s (red solid lines) and 0.001 (blue dashed lines). Simulation parameters: $D_A = 1 \times 10^{-5}$ cm^2 s^{-1}; $S = 1$ cm^2; $A_i + R_i = 1$ mmol L^{-1}. Other parameters in **Experimental** section of the manuscript.

Moreover, the simulations could be also a source of deviations from the analytical equations that could cause the discrepancies shown in Fig. S1. Analytically calculated curves were compared with simulations, revealing that the maximal deviations using a time-step of 0.001 s are approximately 0.5% for the initial points, and for most points, the deviations oscillate between -0.05% and +0.05%, as shown in **Fig. S2.** Therefore, the discrepancies in Fig. S1 are mostly due to the application of numerical semi-operations to the simulated data.

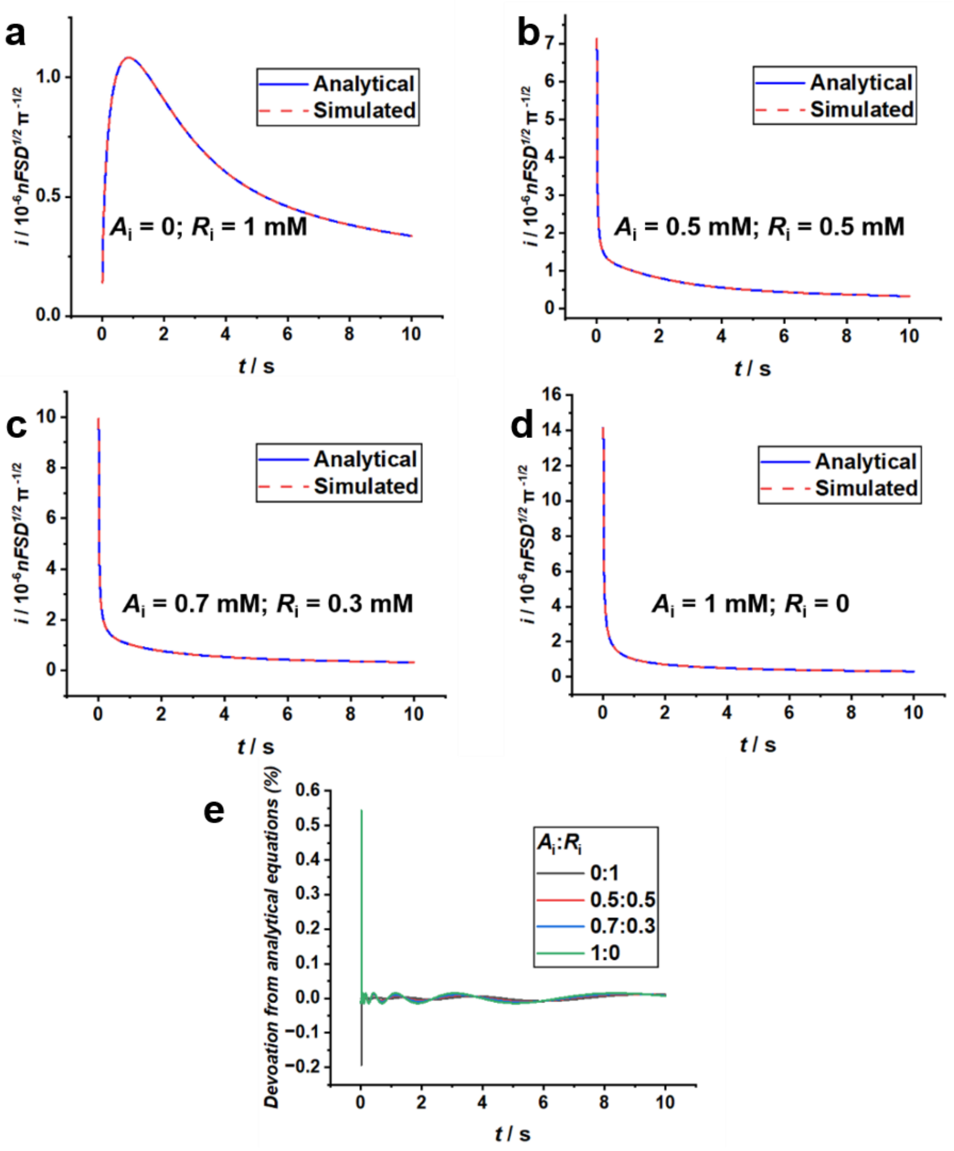

Fig. S2 Analytically calculated (equation 18 from the paper, blue solid line) and simulated currents (red dashed line) considering that the current measurement starts when 0% (a), 50% (b), 70% (c) and 100% (d) of the homogeneous chemical reaction has proceeded. Relative deviation (in %) of simulations from the analytically calculated values (e).

Three different algorithms of differintegration (available in https://github.com/differint/differint?tab=readme-ov-file) were tested on an analytically calculated Cottrell-like decay ($1/\sqrt{t}$) and compared with the values obtained with eL-Chem Viewer. The analytical value of the semi-derivative of such a curve should be 0. However, all the algorithms failed to retrieve this value, as seen in **Fig. S3**.

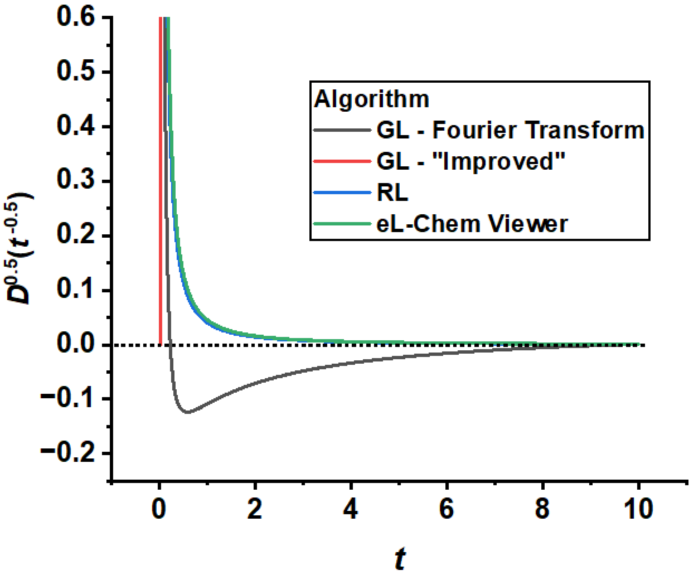

Fig. S3 Semi-derivatives of the function $y = 1/\sqrt{t}$ calculated with GL – Fourier Transform (black line), GL – “Improved” (red line), RL (blue line) and with the eL-Chem Viewer algorithm (green line). The t steps were set as 0.001.

The RL algorithm is based on the Riemann-Liouville definition of differintegral, and is performed with the trapezoidal numerical integration rules. The GL algorithms are based on the Grünwald definition of differintegral. The GL – Fourier Transform is performed with the use of Fourier Transform and GL – “Improved” is performed the the three-point lagrangian interpolation, as described in Chapter 8 of reference 41 of the revised manuscript. The results obtained with GL- Improved and RL algorithms were similar to the ones obtained with eL-Chem Viewer, and the application GL- Fourier Transform algorithm led to even larger deviations from the expected analytical results ($y = 0$).

In **Table S1**, the results of non-linear fits of the semi-derivative chronoamperograms in **Fig. 3c** of the manuscript using equations (23) and (25) are compared. Fits performed with equation (23) give a better estimation of k_f, and the ones made with equation (25) result in more accurate values for the pre-exponential factor $nFSR_0\sqrt{D_\mathrm{A}}k_\mathrm{f}$.

Table S1. Results of the non-linear fits of the graphs in Figure 3c in manuscript. Shaded fit parameters are referent to the equation (23) fits, and non-shaded region is referent to the equation (25) fits.

		Fitted with equation (23)				Fitted with equation (25)		
$A_\mathrm{i}/R_\mathrm{i}$ (set in simulation) [a]	Calculated $nFSR_\mathrm{i}\sqrt{D_\mathrm{A}}k_\mathrm{f}$ (in 10^{-4} A $\mathrm{s}^{-1/2}$) [b]	$nFSR_\mathrm{i}\sqrt{D_\mathrm{A}}k_\mathrm{f}$ (in 10^{-4} A $\mathrm{s}^{-1/2}$)	k_f (in s^{-1})	c from equation (23) / 10^{-6}	R^2	$nFSR_\mathrm{i}\sqrt{D_\mathrm{A}}k_\mathrm{f}$ (in 10^{-4} A $\mathrm{s}^{-1/2}$)	k_f (in s^{-1})	R^2
0	3.051	3.052	1.0001	0.003	> 0.99999	3.052	0.99995	> 0.99999
0.111	2.746	2.759	0.9991	0.040	> 0.99999	2.752	0.99713	> 0.99999
0.250	2.441	2.465	0.99788	0.076	> 0.99999	2.452	0.99366	0.99998
0.429	2.136	2.172	0.99632	0.112	> 0.99999	2.153	0.98926	0.99996
0.667	1.831	1.878	0.99428	0.148	0.99999	1.853	0.98352	0.9999
1.00	1.526	1.585	0.99151	0.184	0.99998	1.554	0.97571	0.99979
1.50	1.220	1.291	0.9875	0.220	0.99995	1.255	0.96448	0.99955
2.33	0.915	0.998	0.98119	0.256	0.99989	0.956	0.94692	0.99901
4.00	0.610	0.704	0.96984	0.291	0.99972	0.658	0.91566	0.99757
9.00	0.305	0.411	0.94333	0.324	0.99905	0.362	0.84459	0.99229

[a] The ratios, from top to bottom, are equivalent to proportions A_i: R_i of 0:1; 1:9; 2:8; 3:7; 4:6; 5:5; 6:4; 7:3; 8:2 and 9:1. [b] Calculated considering n = 1, $F = 96485$ C mol^{-1}, $S = 1$ cm^2, R_i from 0.1 to 1 μmol cm^{-3}, $D_\mathrm{A} = 1 \times 10^{-5}$ cm^2 s^{-1} and $k_\mathrm{f} = 1$ s^{-1}.

In **Fig. S4**, the fitted exponential curves of the graphs shown in **Fig. 3c-d** of the manuscript are shown.

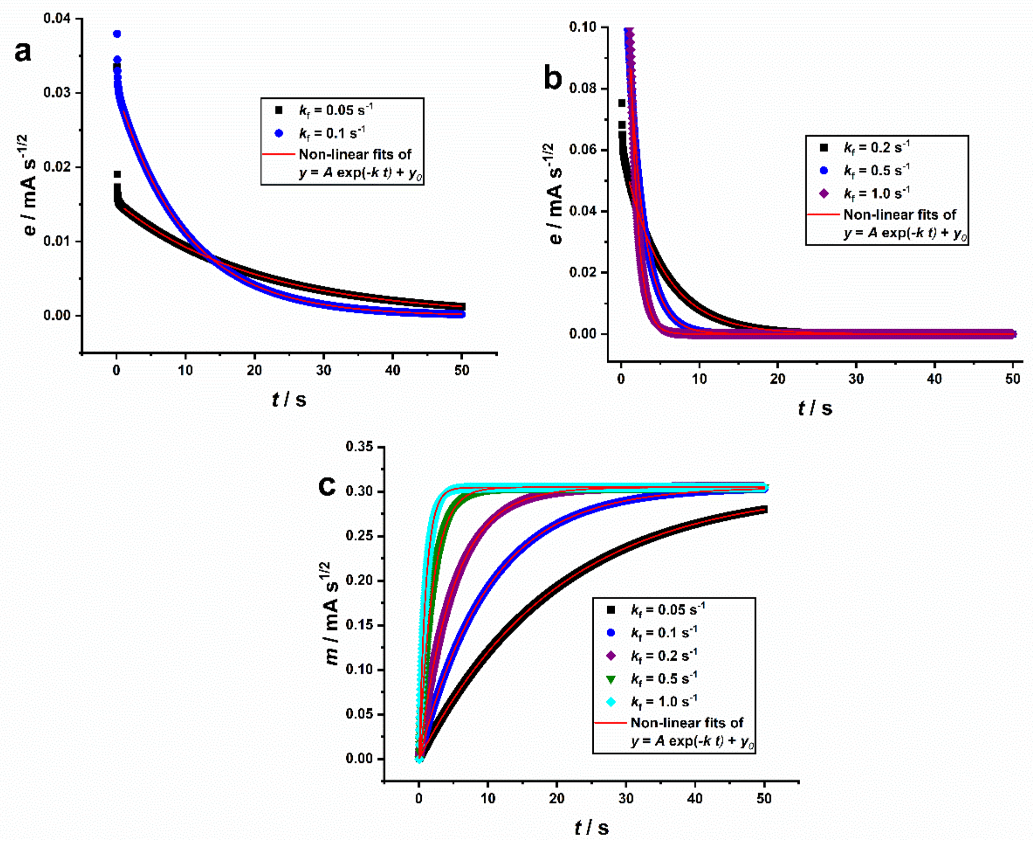

Fig. S4 Semi-derivatives with respect to time of simulated chronoamperograms with k_f set as 0.05, 0.1, **(a)** 0.2, 0.5, 1 s^{-1} **(b)** and without any chemical reaction taking place, with $R_i = 0$ $A_i = 1$ mmol L^{-1}. Semi-integrals are depicted in **(c)**. Non-linear regression of equations (23) and (25) are represented by the red solid lines. Simulation parameters: $n = 1$; $D_A = 1 \times 10^{-5}$ cm^2 s^{-1}; $S = 1$ cm^2; $R_i = 1$ mmol L^{-1}; $A_i = 0$; time step: 0.01 s. Other parameters in **Experimental** section of the manuscript.

In **Fig. S5**, the exponential fits of the graphs shown in Figure 4b-c which led to the fitted k_f displayed in Table 3 of the manuscript are presented. The fitted equations are written in the inset legend, and the initial time for the fits for each k_f, which decreases as k_f increases, is also shown. The fits for the values 0.05, 0.1, 0.2, 0.5 and 1 s^{-1} for k_f started, respectively, at 13.5, 6.9, 2.8, 1.3 and 0.85 s and at 50 s. These values have no special meaning, but they were adequate for the extraction of information in the simulated conditions, as faster chemical reactions will be observed in shorter periods of time and demand the fits to start at shorter times, despite the numerical deviations are concentrated at this portion of the data.

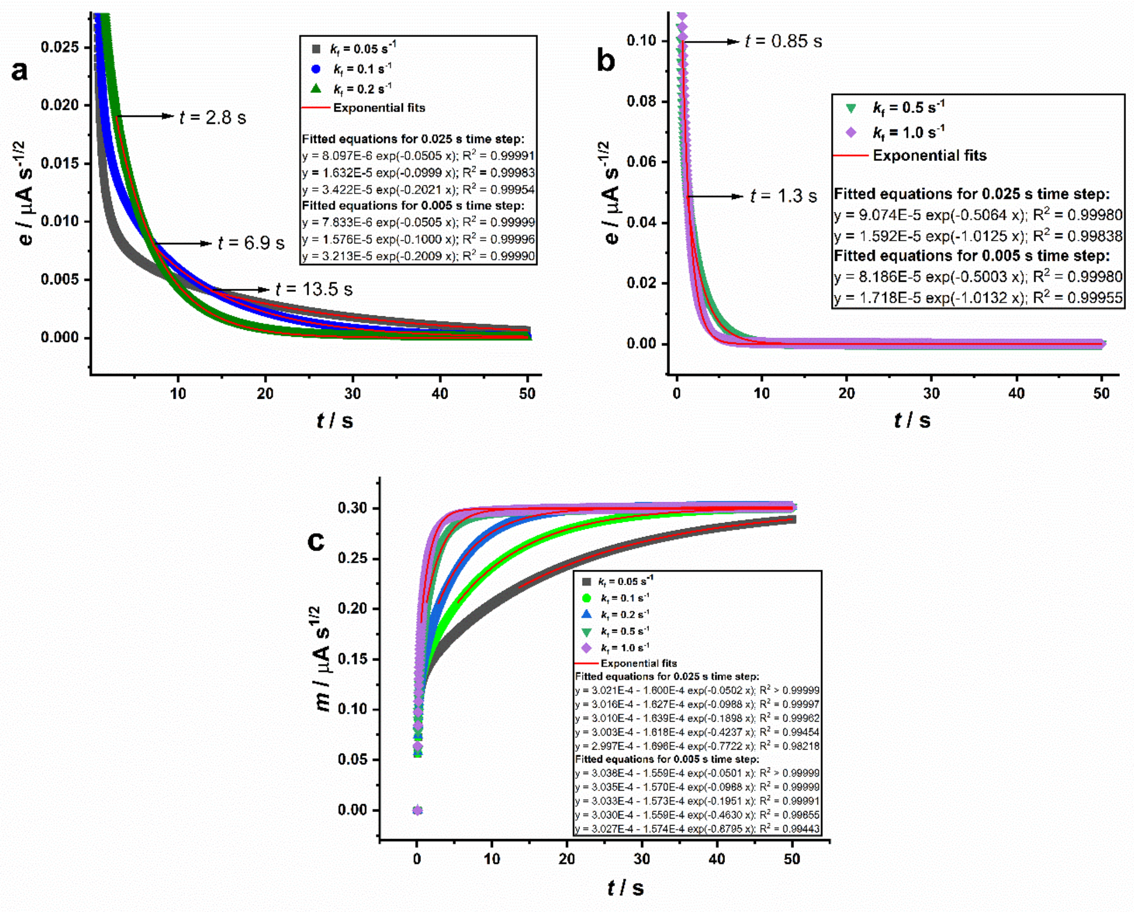

Fig. S5 Semi-derivatives with respect to time of simulated chronoamperograms with k_f set as 0.05, 0.1, 0.2, **(a)** 0.5, 1 s^{-1} **(b)** and without any chemical reaction taking place, with $R_i = 0.5$ $A^* = 1$ mmol L^{-1}. Semi-integrals are depicted in **(c)**. Non-linear regression of equations (23) and (25) are represented by the red solid lines. Inset legend contains the fit Simulation parameters: $n = 1$; $D_A = 1 \times 10^{-5}$ cm^2 s^{-1}; $S = 1$ cm^2; $R_i = 1$ mmol L^{-1}; $A_i = 0$. Other parameters in **Experimental** section of the manuscript.

2. Experimental

The choice of the potential used in the measurement of the chronoamperograms shown in the manuscript was based on the voltammogram shown in **Fig. S6**. The electrochemical reaction observed in the voltammogram may be represented by the following overall reaction:

$$2I^- \rightleftharpoons I_2 + 2e^-$$

The $E_{1/2}$ measured for this reaction at these experimental conditions is 0.498 V vs Ag/AgCl, $KCl_{(sat)}$,. Therefore, by setting the potential at 0.2 V, one can make sure that the concentration of iodine (or tri-iodide) at the electrode surface is virtually null.

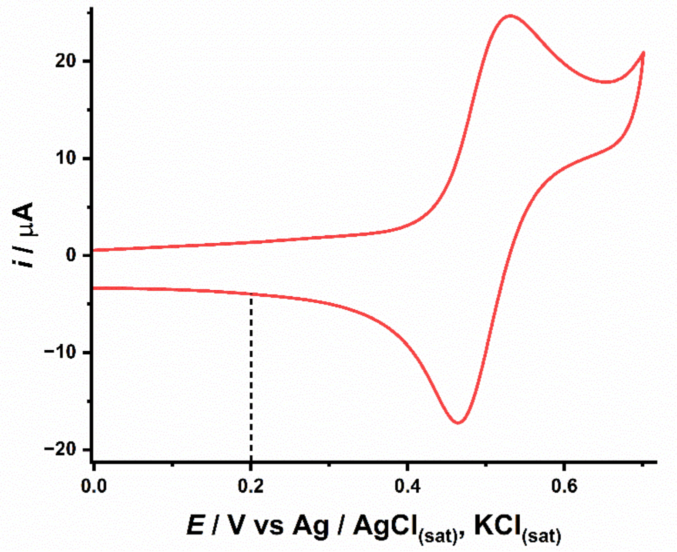

Fig. S6 Cyclic voltammogram obtained with platin electrode in 0.5 mol L^{-1} KCl aqueous solution containing 1.5 mmol L^{-1} of potassium iodide. Scan rate: 0.1 V s^{-1}.

The semi-integral with respect to time of the chronoamperograms presented in **Fig. 6** of the manuscript is depicted in **Fig. S7**. As discussed in the text, this result presents a major deviation from the profiles predicted theoretically and by the simulations due to the radial diffusion contributions to the measured current. This is a common issue that may jeopardize the use of semi-integrals in electroanalytical chemistry without further mathematical treatments. Simonov *et al.* addressed the interference of edge effects in convolution voltammetry for macroelectrodes[1].

The experimental imperfections that affect the initial data points is also a source of error for the semi-integral approach, because, similarly to numerical integration, this semioperation carries deviations from the beginning of the experiment to the calculations made for all the points, potentially affecting values retrieved from the non-linear fits.

Therefore, the semi-derivative approach was chosen for the analysis of the experimental data, leading to rate constants that agreed with previous reports.

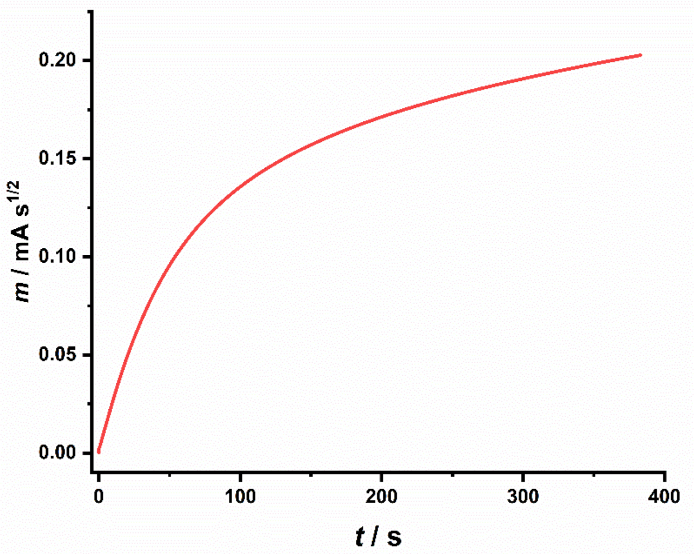

Fig. S7 Semi-integral of a chronoamperogram obtained with Pt disk electrode at 25 °C in a mixture of 0.8 mol L^{-1} of KI, 0.1 mol L^{-1} of HCl and 5.27 mmol L^{-1} of H_2O_2, generating tri-iodide. The applied potential was 0.2 V and the time step was 0.05 s

References

1 A. N. Simonov, E. Mashkina, P. J. Mahon, K. B. Oldham and A. M. Bond, Determination of diffusion coefficients from semiintegrated d.c. and a.c. voltammetric data: Overcoming the edge effect at macrodisc electrodes, *J. Electroanal. Chem.*, 2015, **744**, 110–116.